06JEI00075
1726-2135/1684-8799

www.iseis.org/jei

Journal of Environmental Informatics 8(1) 34-48 (2006)

# A Wintertime Impact of Dilution on Transformation Rate in the Planetary Boundary Layer

A. I. Igbafe[1,2*], L. L. Jewell[2], S. J. Piketh[1] and T. S. Dlamini[1]

[1]Climatology Research Group, University of the Witwatersrand, Private Bag 3, Johannesburg, 2050, South Africa
[2]School of Chemical and Metallurgical Engineering, University of the Witwatersrand, Johannesburg, 2050, South Africa

**ABSTRACT.** The effects of dilution on photochemical reactions of trace gases released from spontaneous combustion processes near open cast coalmines in winter have been examined with a view to assessing the impact of meteorology on atmospheric chemical reactions. Daytime observed gas concentrations vary significantly due to dilution and transformation at average relative humidity of 48.9 ± 4.3 % and temperature of 14.4 ± 0.6 $^{o}$C. Dilution occurred during the day with rise in wind speed. This yielded dilution rate constants of $1.0 \times 10^{-3}$ min$^{-1}$ for CO, $2.5 \times 10^{-3}$ min$^{-1}$ for NO, $1.9 \times 10^{-3}$ min$^{-1}$ for $NO_2$, $8.4 \times 10^{-4}$ min$^{-1}$ for $H_2S$, $9.8 \times 10^{-4}$ min$^{-1}$ for $SO_2$ and $1.6 \times 10^{-3}$ min$^{-1}$ for $O_3$. $H_2S$ and $SO_2$ were observed to exhibit very close resemblance in diurnal variations. The average daytime and night time concentrations of the observed $H_2S$ were 31.5 ± 13.4 ppb and 171.7 ± 15.9 ppb and 31.6 ± 13.2 ppb and 128.5 ± 18.1 ppb for $SO_2$. Chemical reaction rates were evaluated over a temperature range between 0 and 20 $^{o}$C and mean surface pressure of 850.4 ± 2.7 mbar for the trace inorganic gases. Over this temperature range and surface pressure, transformation rates of $SO_2$ and $H_2S$ are 0.023 %$\cdot h^{-1}$ and 0.008 % $h^{-1}$ respectively. The pre-exponential rate constants of the gaseous species are $k_{H_2S} = 6.65 \times 10^{-3}$ L $\mu g^{-1}\cdot$min$^{-1}$, $k_{SO_2} = 1.67 \times 10^{-3}$ $L\cdot\mu g^{-1}\cdot$min$^{-1}$, $k_{NO_2} = 4.7 \times 10^{-3}$ min$^{-1}$, $k_{NO} = 1.27 \times 10^{-2}$ min$^{-1}$and $k_{O_3} = 5.49 \times 10^{-1}$ $L\cdot\mu g^{-1}\cdot min^{-1}$. The energy of activation of the gaseous species are $E_A$ / R was approximately 317 K for $H_2S$, 696 K for $SO_2$, 258 K for $NO_2$, 292 K for NO and 1,684 K for $O_3$.

*Keywords:* Coalmining, combustion, dilution, meteorology, photo-oxidation, trace gas

## 1. Introduction

Several air pollutants that prevail in the cities and townships of developing communities consist of the trace gaseous compounds. In the atmosphere these compounds undergo a transformation from gas to particles resulting in smog formation (Terblanche et al., 1993; Blanchet, 1994; Andrews et al., 2004). On the South Africa Highveld, anthropogenic gases released from spontaneous combustion in coalmines have significantly increased the tropospheric air pollutant load (Held et al., 1996).

Within southern Africa, coal and its products are the major energy source for heating, electricity generation and industrial applications. The Witbank area of the Highveld (Figure 1) is a major coal-producing area in South Africa. Of significant interest is that Witbank coalfields contain low-grade bituminous coal suitable for syngas fuel and electric power production (Edna, 1957; Barker and Associates, 1985; Gayer and Harris, 1996; Snyman et al., 1990). Several studies of atmospheric pollutant released from coal-fired processes have been undertaken (Dittenhoefer and De Pena, 1978; Rodhe, 1978; Fugas and Gentillizza, 1978; Santos et al., 2004; McGonigle et al., 2004).

Air mass transport is controlled by the variability of meteorological parameters. These parameters also alter the state of atmosphere that result in dilution and chemical transformation. Dilution in the atmosphere refers to the introduction of cleaner air (inert of the reacting species) as a result of rise in wind speed into a reaction mixture which reduces the concentrations of the reacting species. Several factors may affect the dilution process of concentrated surface emissions. These include the diluents source type and emission strength, the physical and chemical nature of the emissions, rate of inflow and outflow of the air-mass and to a significant extent the meteorological variables in the location. On the other hand chemical transformation involves the change in chemical form, structure and energy content of reactive species when subjected to specific temperatures and pressures. In the atomsphere chemical transformations are influenced by meteorological parameters such as ambient temperature, solar radiation (Calvert et al., 1978; Pienaar and Helas, 1996; Warneck, 1999) and relative humidity (Moller, 1980).

Within the troposphere, the oxidation rate $SO_2$ ranges between 0.7 and 8 percent per hour (Miller, 1978; Seinfeld and Pandis, 1998). The variation in rates is as a result of the complexity of atmospheric reactions, variations in meteorological parameters and the methodology by which the reaction kinetics was conducted (Gillani et al., 1978). Some techniques applied include passive sampling at constant time intervals of reacted compound obtained from adsorbent impregnated with a reaction quench (Gillani et al., 1978; Gillani and Wilson, 1983). Others include atmospheric conditions simulated in laboratory studies (Carmichael and Peters, 1984). The use of

* Corresponding author: anselm@crg.bpb.wits.ac.za

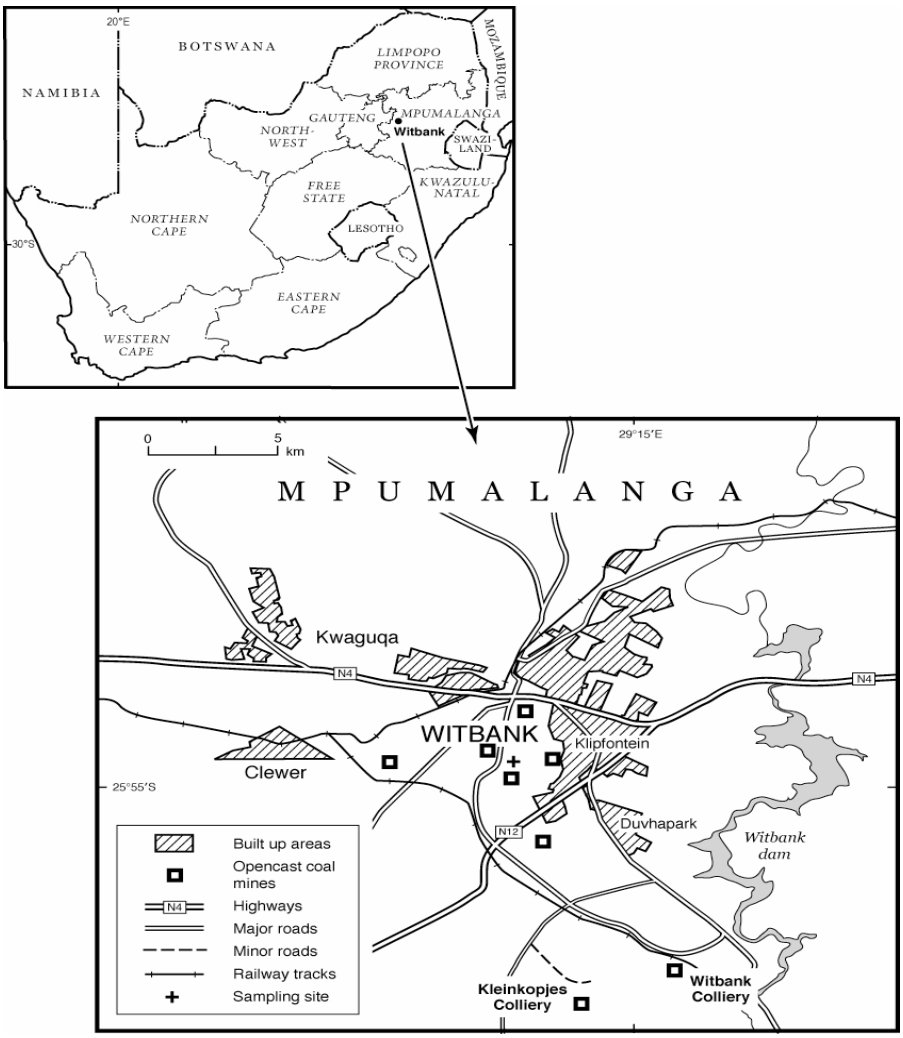


**Figure 1**. Map of South Africa and an enlargement of the Witbank area, sampling site and open cast coalmines within Mpumalanga Province.

passive method significantly allows for deposition rates than transformation rates, since chemical reaction rates are a function of seconds, minutes and hours, while the laboratory studies attempt to simulate the real situation, this do not exactly reflect the abrupt variations in meteorology of the atmosphere. Both techniques have been applied over the South African environment for photochemical, homogeneous and heterogeneous reactions (Breytenbach et al., 1994; Pienaar and Helas, 1996).

In an open atmosphere, it is difficult to discriminate between homogeneous and heterogeneous reactions, as all processes occur simultaneously under the influence of surface meteorology (Liberti et al., 1978 and Charlson et al., 1974). A number of studies have been carried out on photochemical oxidation of trace gases (Cox and Sandalls, 1974; Calvert et al., 1978; Chisaka, 1984; Pienaar and Helas, 1996). However, not much has been reported with respect to modelling the reaction rates relative to dilution rate for the daytime reactions. Trace gases released from partial or complete combustion processes in open cast coalmines at Witbank were observed to experience dilution during photochemical oxidation. Similar to any chemical reaction, the rates depend on the meteorological conditions in the planetary boundary layer and the nocturnal concentrations of the emitted gases. To ascertain that source concentration was utilised for the reaction kinetic model, concentration distribution as a function of the wind directional sectors is essential.

On a local scale, the wind direction may influence the air quality at a particular monitoring site. The air transport regimes are useful in determining the pathways travelled by pollutants from their sources thereby providing a measure for source-site targeting (Timko and Derrick, 1989; Davison and Hewitt, 1997). In this paper, the contribution of meteorology to concentration variations has been considered to provide an

understanding of ambient concentration variations of several photo-chemically propagated transformations with increasing wind speed. Consequently to establish a representation of the chemical transformation rates of five trace gases observed around Witbank open cast coalmines, CO is used as a tracer gas for air mass dilution determination. Studies have shown that CO time based trends are the most accurate indicators of spontaneous combustion (Timko and Derrick, 1989; Davison and Hewitt, 1997).

The trace gases considered in this study were $SO_2$, $H_2S$, NO, $NO_2$, $O_3$ and CO. $H_2S$ is thermally oxidised to $SO_2$ in the atmosphere (Eggleton and Cox, 1978). $SO_2$ is converted into sulphate through several reaction mechanisms (Cox and Sandalls, 1974; Calvert et al., 1978; Moller, 1980; Stockwell, 1986; Walcek et al., 1986; Pienaar and Helas, 1996; Warneck, 1999). The NO is predominantly formed during combustion of fossil fuels while the oxidation of NO produces $NO_2$ in the atmosphere (WHO, 1979; Tang et al., 1981; Seinfeld and Pandis, 1998; Warneck, 1999). When volatile hydrocarbons react with these oxides of nitrogen, $O_3$ is formed (WHO, 1979; Pienaar and Helas, 1996; Warneck, 1999). CO is a product of the incomplete combustion of fossil fuels and carbonaceous compounds (WHO, 1979; Warneck, 1999). It may be considered as an inert relative to the other trace gases because it has a characteristic lifetime of between 1 and 4 month in the at- mosphere (Seinfeld and Pandis, 1998).

Chemical transformations depend on the temperature and pressure of the system while the rates of reaction depend on the temperature and the concentration of the reactant species (Smith et al., 1996). Photochemical oxidation is a well established mechanistic path-way of transformations for a variety of atmospheric pollutants. It is different from other reaction mechanisms because a photon (a light energy associated with a particular wavelength released to initiate a reaction) is one of the reactants (Seinfeld and Pandis, 1998). In the atmosphere, several chemical reactions are initiated and propagated by sunlight with ray intensity expressed in terms of the forward or reverse rate constant (Chisaka, 1984). Most atmospheric transformations are considered irreversible since the equilibrium product concentration necessary for reversibility are trivially produced. In addition some products act as intermediate reactants for the formation of other products. The equilibrium concentration ratio of $SO_2$ to $SO_3$ is about $8 \times 10^{11}$ in the air at 25°C and 1 atmosphere (Pienaar and Helas, 1996; Seinfeld and Pandis, 1998). Therefore reaction rates may be expressed in terms of either the disappearance of reactants or the formation of products or the combination of both in the case of reversible reactions (Levenspiel, 1999). The method adopted in this study is the differential method of data analysis. This method uses a differential rate equation which is evaluated for all the terms as well as the derivative term - d$C$/d$t$ (change in concentration reactant with respect to time). It also tests the goodness of the fit with experimental observations (Levenspiel, 1999).

The reaction rate, $r_i$ for the disappearance of a limiting reactant, $i$ based on the differential method with the assumption of constant-density reacting fluid mixture is expressed as:

$$r_i = \frac{1}{V}\frac{dN_i}{dt} = \frac{d(N_i/V)}{dt} = \frac{dC_i}{dt} = -kC_i^n \quad (1)$$

where $r_i$ ($mol{\cdot}L^{-1}\ s^{-1}$) is the rate of disappearance of the reactant, $C_i$ ($mol{\cdot}L^{-1}$) is the concentration of the reactant $i$, $n$ (unit less) is the order of reaction, and $k$ is the reaction rate constant. $k$ is expressed as $s^{-1}$, for first order reactions and $L{\cdot}mol^{-1}{\cdot}s^{-1}$ for second order. Taking logarithms of both sides of equation (1) gives:

$$-\ln r_i = n \ln C_i + \ln k \quad (2)$$

A plot of ln $r_i$ against ln $C_i$ from equation (2), gives a straight line with a slope equal to the reaction order, $n$ and an intercept equal to the reaction rate constant, $k$ (Levenspiel, 1999; Perry and Green, 1999). The rate constant, $k$ which is temperature dependent for a specific pressure, is defined by the Arrhenius equation (3):

$$k = k_\infty \exp\left[-\left(\frac{E_A}{R}\right)\frac{1}{T}\right] \quad (3)$$

where $k_\infty$ is the pre-exponential factor with same unit as $k$, $E_A$ is the energy of activation in $kJ{\cdot}kg^{-1}$ and $R$ is the universal gas constant. $T$ is the temperature at which the reaction occurred in Kelvin. Equation (3) fits experiments well over a wide temperature range and is the best model approximation to true temperature dependency (Levenspiel, 1999; Perry and Green, 1999). At two different temperatures, for the same compound, equations (2) and (3) combine to give:

$$\ln\left(\frac{r_2}{r_1}\right) = \ln\left(\frac{k_2}{k_1}\right) = \frac{E_A}{R}\left(\frac{1}{T_1} - \frac{1}{T_2}\right) \quad (4)$$

where, $r_1$ and $r_2$ are reaction rates at temperatures $T_1$ and $T_2$ with rate constants $k_1$ and $k_2$ respectively.

## 2. Methodology

Ambient air sampling was conducted at the Witbank area (Figure 1) on the South African Highveld on a location midst of several open cast coalmines. Sampling was conducted on a continuous basis for one month with weekly instrument calibration using high response time thermo environmental analysers on a ten-minute time average. In addition meteorological parameters were measured also on a ten-minute time average.

Meteorological data was analysed in order to establish their contributions to the atmospheric conditions. Air mass dilution was established from the moment daytime accumulation of ozone concentration started to decrease while at the

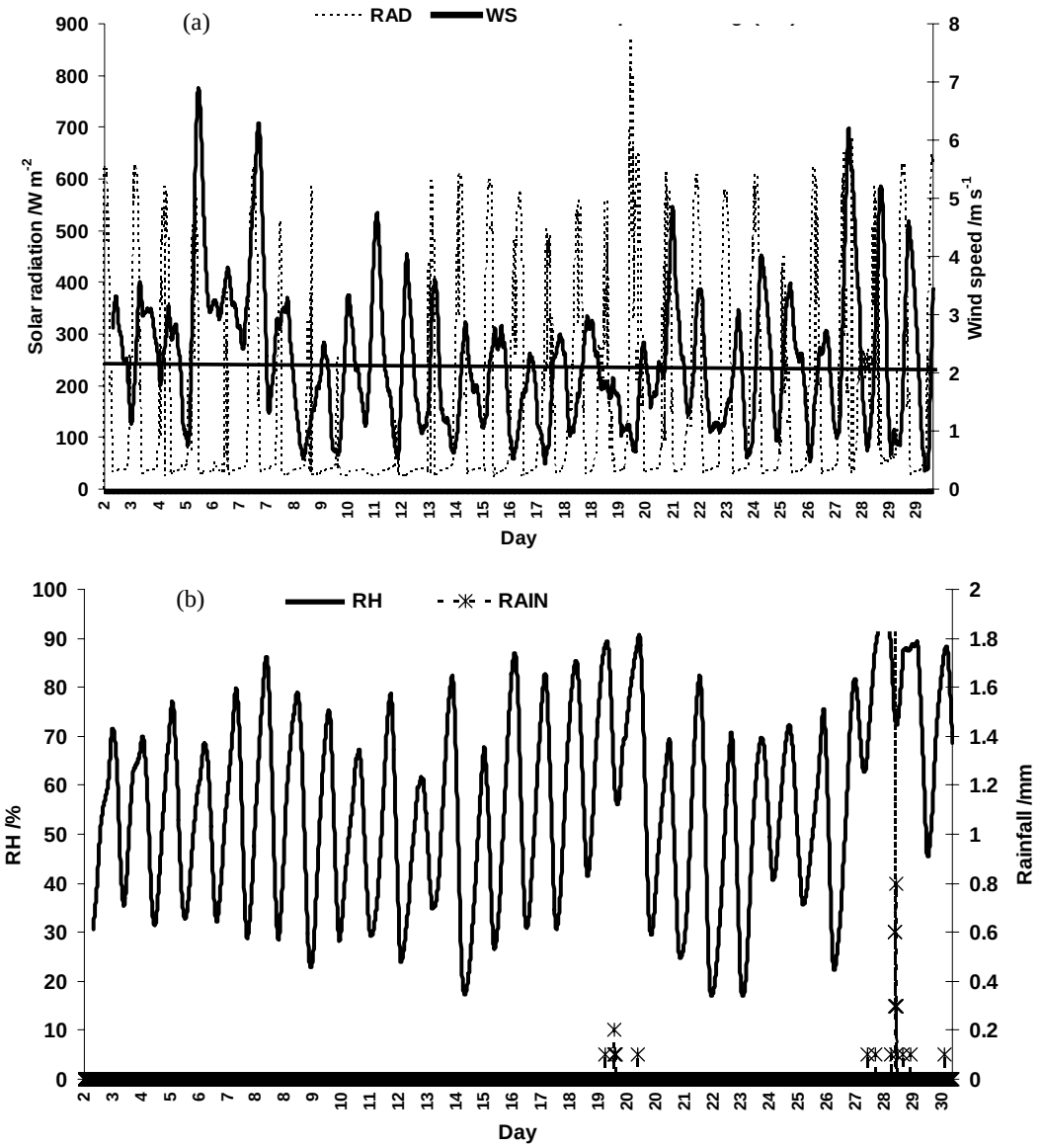


**Figure 2**. (a) Variations of solar radiation and wind speed measurements at Witbank in June 2004. The line with constant wind speed of 2ms$^{-1}$ indicate calm conditions; (b) Variations in relative humidity (RH) and rainfall measurements at Witbank in June 2004.

same time wind speed was increasing. The dilution process was complete from the moment the growth in ozone concentration recommenced. Over this period, the CO (considered as inert) was used as a tracer to determine the amount of diluent air that would have been introduced to reduce its nocturnal concentration. The same amount of air-mass, producing the same dilution factor for all components of the mixture, was applied to the other trace gases in order to determine the corresponding dilution rates. The decrease in concentration prior to the dilution was attributed to chemical transformation.

Over the duration of wind speed increase, dilution was presumed occurring simultaneously with chemical transformation. The feasible period of establishing the occurrence of chemical reactions was during the ozone production after sunrise and reduction after sunset. Chemical reaction rates were established by formulating simple kinetic models from measured data of the trace gases. The order of reaction and rate constant were determined from the rate model expressions. The transformation rate was based on the assumption that the reactant initial concentration was the nocturnal gas concentration.

Photochemical transformations were assumed to be the

dominant reaction mechanism by which the trace gases were consumed. This reaction mechanism is enhanced by the presence of sunlight and oxidising agents in the reaction mixture. Theses agents of oxidation are highly selective to specific chemical reactions and conditions. Selectivity is used to describe the degree to which a particular reaction predominates over competing side reactions. If a chemical reaction yields two products A (desired) and B (undesired), the selectivity of product A is the mole ratios of A relative to B and vice versa, such that the summation of the selectivities of all products is 100% (Felder and Rousseau, 2000).

The reaction rates were established on the assumption of a constant-density fluid mixture (daytime mixed layer height). The daytime mixing height $h_n$ was calculated utilizing morning potential temperature soundings before sunrise as well as the hourly changing surface heat flux for the day time mixing heights as described in Holtslag and Van Ulden (1983); Van Ulden and Holtslag (1985) by using convective the boundary layer parameters evaluated from works of Oke (1987); Panofsky and Dutton (1984); Wyngaard (1988); Deardorff et al. (1980); Garratt, (1992); Hanna and Paine, (1987); Hanna and Chang, (1993) and Cimorelli et al. (2004). The stable (night time) mixing layer height, $h_s$ was determined based on works of Zilitinkevich (1972) and Venkatram (1980a, b, c).

## 3. Sampling Description

Sampling was undertaken during winter between 2 and 30 June 2004 in Witbank, an area located in the northern part of the South Africa Highveld (Figure 1). It is a relatively flat topographical terrain with a few rolling hills. The vegetation is a sparse and varied grassland type. It is an open area that allows for effective diffusion and mixing close to the surface. Meteorological parameters consisting of ambient temperature, pressure, wind speed and direction, solar radiation, relative humidity and rainfall were measured continuously on a ten-minute average.

The sampling site was a ground-based air quality monitoring station equipped with instruments to measure ambient trace gas concentrations for $H_2S$, $SO_2$, $O_3$, NO, $NO_2$ and CO. The sampling site was situated in an area about 1500m ASL on S25°59'07" E29°13'23" (Figure 1) surrounded by a number of active open cast coalmines. The closest open cast coalmines to the sampling site were approximately 1 km and 2 km away in the south and north–westerly directions respectively. Each of the surrounding coalmines had a surface area of between 0.12 and 0.18 $km^2$.

The trace gases were measured using Thermo Environmental instruments. Measurements of $SO_2$ were conducted using a model 43C $SO_2$ pulse analyser. A detailed description of the instrument operation is given in Dittenhoefer and De Pena, (1978). $H_2S$ was measured using a model 340 $H_2S$ catalytic converter coupled to an $SO_2$ model 43C pulse fluorescence analyser. The catalytic converter oxidises all $H_2S$ to $SO_2$ and the output gives the total $SO_2$ ($SO_2$ from $H_2S$ plus $SO_2$ in air) content in the sampled air. The $H_2S$ concentrations were calculated by subtracting the $SO_2$ concentrations measured by an $SO_2$ analyser from values measured by the $H_2S$ – $SO_2$ combined monitor and analyser. Other instruments employed for the monitoring include: the Model 42C trace level $NO/NO_2/ NO_X$ analyser for monitoring and measuring of oxides of nitrogen, the Model 49C trace level $O_3$ analyser for ozone and the Model 48C trace level CO analyser for carbon monoxide. The time taken for sampling and analysing a sample in the instruments was 60 seconds. The measured concentrations were recorded on a 10-minute average basis. This was to correlate concentrations with measured metrological data.

## 4. Result Analysis

### 4.1. Meteorological Variations

Over the area at Witbank sunrise occurred between 05:00 and 06:00 in the June 2004. In most of the period during sampling, the atmosphere was between calm to stable conditions with a few neutral conditions on the first and last week of the June 2004 (Figure 2a). There was a clear indication of diurnal wind variations throughout the sampling duration defined by a morning increase reaching a peak at midday followed by gradual reduction as the sun sets. It appears that most of the days during sampling were cloudless with the exception of days 6, 8, 17 and 25 that were significantly low in solar. While days 9 and 13 appeared to be partially cloudy at certain times of the day hence the slim appearance of solar radiation, overcast conditions was observed between the June 10 and 12. During the sampling period only slight rainfall was observed on June 28 with drizzles on between June 18 and 20 as well as 27 and 30 (Figure 2b). Except for the rain days, the relative humidity was consistent over a particular range between 20 and 90%.

### 4.2. Wind Effect on Concentration Distribution

A simple representation of pollutant distribution resulting from wind action is the pollution rose (Figures 3a to 3f). In this plot the dotted lines indicate the mean concentrations for the various wind direction over the sampling duration. The length of the straight line shows the frequency of wind from a particular direction, while the thickness of the line indicates the frequency of occurrence of particular concentration range for a particular wind direction.

The winds from north-westerly and southerly were predominant at the sampling location throughout the month of June (Figures 3a to 3f). Maximum CO concentrations were observed from the north-westerly to east (clockwise) sector and the south-westerly to south-easterly sectors (Figure 3a). These directional sectors coincided with the locations of the coalmines closest to the sampling site (Figure 1). Therefore CO is most likely an outcome of the spontaneous combustion from the nearby open cast coalmines. It appears from the dotted lines that CO is uniformly distributed over the area. This may be due to its long atmospheric lifetime of between 1 and 4 months (Seinfeld and Pandis, 1998). Equally very high con-

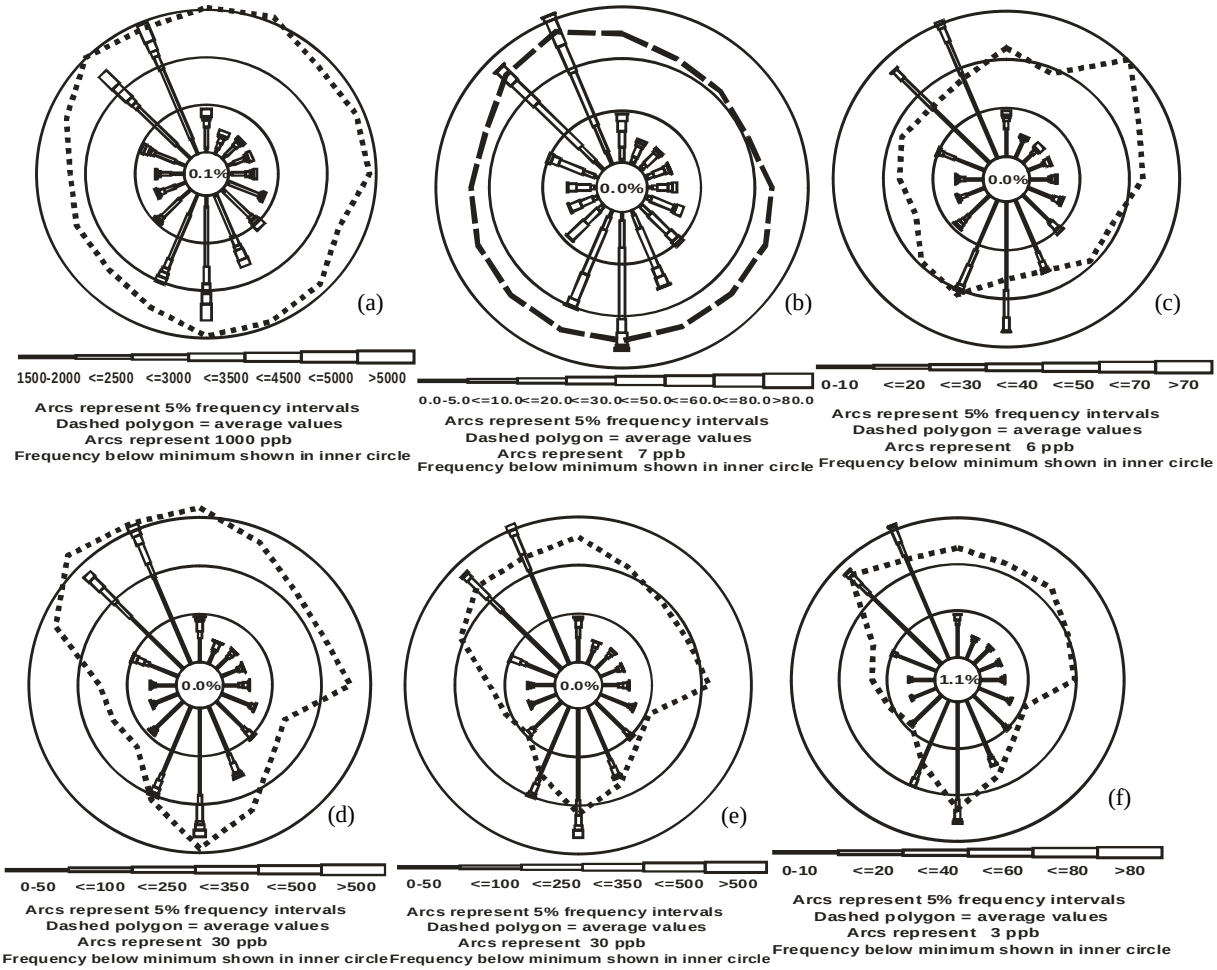


**Figure 3.** Mean CO (a), $O_3$ (b), $NO_2$ (c), $H_2S$ (d), $SO_2$ (e) and NO (f) concentration distribution within open cast coalmines at Witbank in June 2004.

centrations of $H_2S$, $SO_2$ and NO (Figures 3d to 3f) were observed from the wind directional sectors similar to the CO source area. Hence it be ascertained that the same source for CO is responsible for the gaseous emissions. It is well understood that $O_3$ and $NO_2$ produced predominantly due to chemical reactions with other atmospheric compounds; hence no specific emission source may be attributed to their presence (Figures 3b and 3c). Consequently the average concentration shown by the dotted is uniformly distributed.

At sunrise as the nocturnal temperature inversion aloft it is expected that convective eddies mix the nocturnal concentrate towards the surface since upward diffusion is prevented (Briggs, 1969; Oke, 1987). This process in addition with low convective mixing height during winter at Witbank should significantly increase ground level concentrations. But over the sampling area the reverse was observed as wind speed increases between 06:00 (1.35 $m{\cdot}s^{-1}$) and 11:00 (3.68 $m{\cdot}s^{-1}$) by about 56.1% (Figures 4a to 4c). The decrease in concentration was significantly observed with CO and NO diurnal variations. While with respect to altering transformation, concentration reduction was clearly shown by $O_3$ reduction after sunrise. It was assumed that the rise in the morning wind speed introduces cleaner air into the trace gas mixture resulting in dilution. Thereafter with steady wind speed, photochemical transformation processes became dominant.

### 4.3. Diurnal Variations

The observed ambient concentration variations are significant influenced by surface meteorological parameters (Table 1). Throughout the sampling period, the concentrations of all the trace gases exhibited a regular cyclical diurnal pattern. The average nocturnal CO concentration decreases due to the wind effect from about 4,669.4 ppb to 2,456.5 ppb, between 06:00 and 15:00 (Figure 4a). As sunset approaches, the concentration accumulation recommenced. Such a concentration growth occurred gradually between 15:00 to 06:00 increasing

**Table 1.** Average ± Standard Deviation Meteorological Parameters

| | Wind Speed ($m \cdot s^{-1}$) | Ambient Temperature ($^oC$) | Relative Humidity (%) | Solar Radiation ($W \cdot m^{-2}$) | Surface Pressure (mbar) |
|---|---|---|---|---|---|
| Daily | 2.6 ± 0.6 | 8.2 ± 0.7 | 60.2 ± 4.8 | 131.8 ± 37.9 | 850.4 ± 2.7 |
| Daytime | 2.9 ± 0.5 | 14.4 ± 0.6 | 48.9 ± 4.3 | 244.9 ± 24.7 | 852.8 ± 0.3 |
| Daily Minimum | 0.7 ± 0.5 | 0.7 ± 0.2 | 29.4 ± 9.1 | -0.4 ± 0.1 | 848.8 ± 3.0 |
| Daytime Minimum | 0.8 ± 0.5 | 2.6 ± 1.1 | 27.2 ± 5.0 | 8.6 ± 0.7 | 851.0 ± 3.0 |
| Daily Maximum | 4.2 ± 1.5 | 16.1 ± 1.8 | 87.2 ± 7.9 | 551.6 ± 81.1 | 852.3 ± 2.8 |
| Daytime Maximum | 5.8 ± 1.3 | 19.4 ± 2.2 | 86.7 ± 7.8 | 516.9 ± 55.9 | 854.3 ± 3.0 |

pollutant within the planetary boundary layer.

The diurnal pattern exhibited by $H_2S$ and $SO_2$ are similar (Figure 4b). Between 22:00 and 06:00 the concentrations increased reaching a maximum of 225.1 ppb and 162.2 ppb of $H_2S$ and $SO_2$ respectively. These events are due to the result of source strength variation accompanied by wind directional responses. The concentration increases between 06:00 and 08:00, as a result of the increased traffic in the mines as well as the early morning mine-rocks blasting operations; a steep decline in both species was observed between 08:00 and 10:00, yielding about 30.7 ppb $H_2S$ and 28.3 ppb $SO_2$. This reduction, which amounted to about 80% of their night time concentrations, occurred after two hours from the time when wind speed increase was initiated. The reduced concentration remained steady even at wind speed as well as with decreasing wind speed after 15:00. As a result, this decline was attributed to combination of dilution and photochemical transformation processes. At night time about 22:00 concentrations gently started to accumulate.

The oxides of nitrogen exhibited different diurnal characteristics during the sampling (Figure 4c). Throughout the sampling period NO formation occurs between 04:00 and 06:00 due to spontaneous combustion from the coalmines. At 06:00, NO reduction began due to sunrise, resulting in photo-oxidation processes. This decline proceeded up to 11:00 reaching a minimum of about 5 ppb after decreasing about 80% of the night time concentration. The reduced concentration remained steady up to 22:00 when both wind and photochemical effects were insignificant and accumulation resumed. It is well understood that $NO_2$ is mainly the result of photo-oxidation of NO in air (Pienaar and Helas, 1996; Seinfeld and Pandis, 1998; Warneck, 1999). As a result, the night time $NO_2$ would remain stable except for the interferences from atmospheric stability. While in the daytime it is used up during the production of the photochemical oxidants. The observed $NO_2$ concentration apparently remained stable through the night thereafter it decreased gradually between 09:00 and 11:00 by about 39% of average nocturnal value reaching a minimum of about 6.8 ppb (Figure 4c). The time of reduction corresponds to the frame of wind speed rise hence the concentration disappearance is possibly the result of air dilution. After 12:00, $NO_2$ accumulation resumed.

$O_3$ is a strong oxidizing compound in the atmosphere. The formation of $O_3$ is as a result of the disappearance of $NO_2$ thereby making $NO_2$ an oxidant precursor. The production of $O_3$ is also propagated by the presence of sunlight (Pienaar and Helas, 1996). The characteristic pattern shown by ozone was a stable night time value up till about 07:00. This was followed by an increase between 07:00 and 09:00 reaching a maximum of 25.8 ppb as a result of photochemical oxidation processes. This increase was interfered between 09:00 and 11:00 creating a reduction to as low as 12.8 ppb removing about 17% of the initially attained maximum concentration. This reduction was ascribed to the dilution since the introduction of oxygen-rich air should contribute to increased oxidation rather than concentration reduction. Therefore the $O_3$ disappearance was due to air dilution suppressing photochemical reaction. Thereafter between 10:00 and 15:00, photochemical oxidation exceeded dilution, hence ozone accumulation (Figure 4c). After 15:00 towards the evening as the sun set, with a subsequent reduction in the intensity of the solar radiation, a rapid decrease in $O_3$ was observed up till 17:00, followed by a gentle reduction reaching a minimum of 10.8 ppb at 23:00.

### 4.4. Effect of Dilution on Emitted Gases

The disappearances of the measured trace gases between 06:00 and 15:00 is partly associated with dilution resulting from increased wind speed bringing excess clean air into the observed gaseous mixture and partly due to transformations. The decrease in CO has been completely ascribed to dilution and not chemical transformation. This is because it is partially inert, since it has a long residence time in the atmosphere, hence CO released within 24-hour does not participate in chemical transformation, for this reason it was used as a tracer gas relative to $H_2S$, $SO_2$, NO, $NO_2$ and $O_3$.

Daily reduction in CO concentration occurred between 06:00 and 15:00 corresponding to the period of rise in wind speed (Figure 4a). The concentration reduction commenced at 06:00 on a gentle gradient up till 15:00. Since the reduction coincided with the rise in wind speed, it was attributed to dilution. The dilution observations was also significantly noticed between 09:00 and 11:00 for $O_3$ (Figure 4c). In this event $O_3$ decreased from about 26.2 ppb to 19.3 ppb between 09:00 and 11:00, as the increase in wind speed approached its peak. The distortion by the morning increase in wind speed occurred within two hours after which the concentration accumulation resumed. The $O_3$ reduction prior to sunrise was essentially concentration fluctuations in background, while during the day

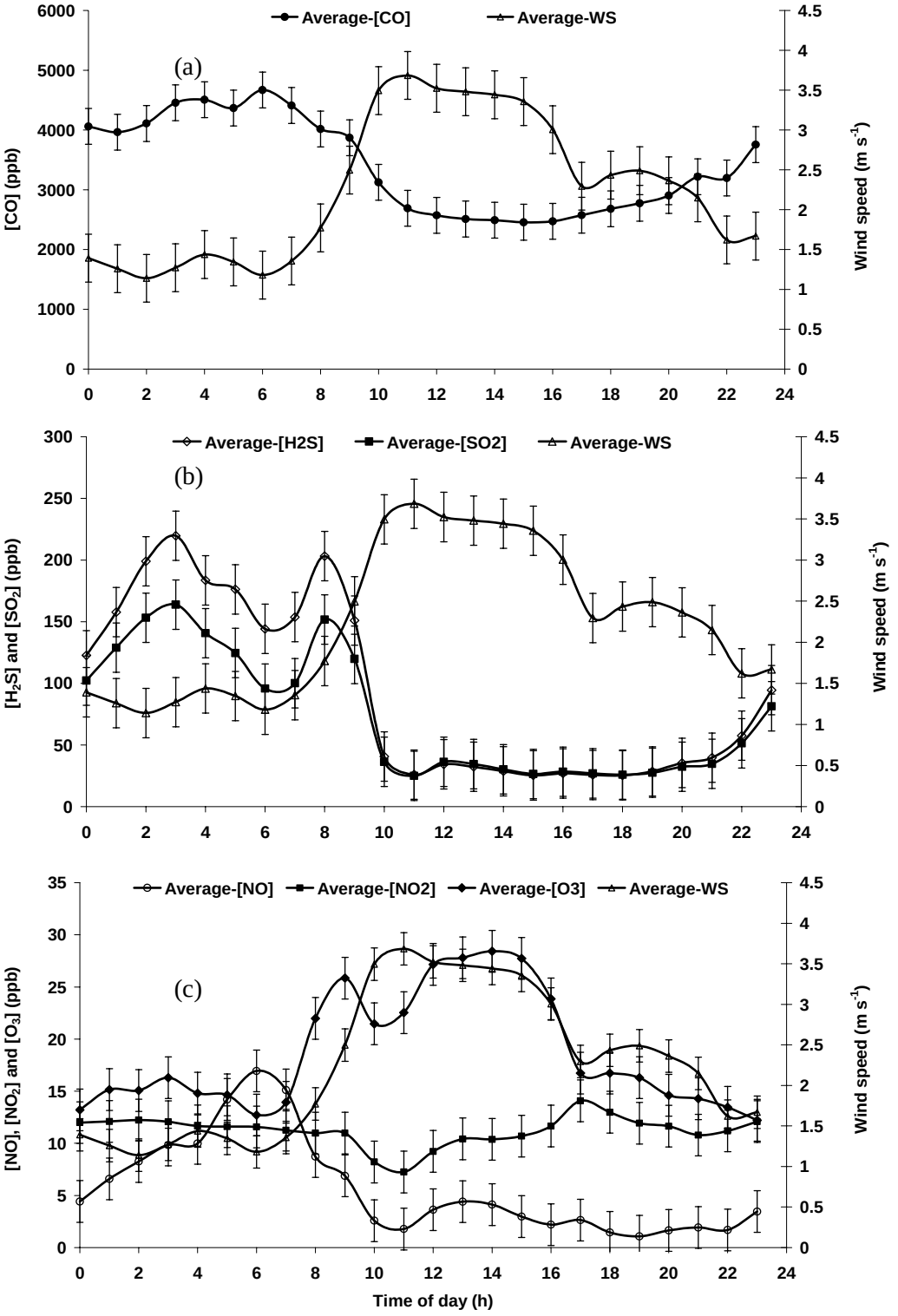


**Figure 4**. Diurnal variations of ambient CO (a), $H_2S$ & $SO_2$ (b) and NO, $NO_2$ & $O_3$ (c) concentration with wind speed in the coalmining area of Witbank obtained as an average of all observations in June 2004.

the formation and reduction are ascribed to chemical transformations with the presence of solar radiation.

Consequent to the observations of CO and $O_3$, concentration reductions between 06:00 to 10:00, were used to establish the dilution rates for the other trace gases. With $H_2S$ and $SO_2$ concentration reductions, disappearances are attributed to both dilution and transformation. Prior to 09:00 chemical transformation dominated concentration reduction as shown with $O_3$ disappearances and between 09:00 and 11:00 dilution was the predominant controlling factor. Hence the reduction of $H_2S$ from 140 ppb to 20 ppb and $SO_2$ from 110 ppb to 19 ppb between 09:00 and 11:00 was attributed to dilution as cleaner air containing little or none of the sampled pollutant was introduced into the mixture. After 11:00, the concentrations were reduced to values insufficient to contribute to a chemical reaction. As a result of these two processes, established chemical transformation rates are expressed as rates affected by dilution.

Between 06:00 and 11:00, a decrease in NO concentration was observed. One would expect this to result in increasing $NO_2$, although a very slight increase was observed at 06:00 followed by a little reduction in $NO_2$ between 09:00 and 11:00. This suggests that the NO was partially converted to $NO_2$, but that the dilution masked the net increase in $NO_2$ from NO oxidation.

The rate of dilution of the various gases was determined from the daytime concentration changes between 09:00 and 10:00 using similar approach described in Seinfeld and Pandis, (1998). For CO dilution, the rate gradients defined by the change in concentration with respect to time of occurrence were obtained from the plot of concentration with time (Figure 5) derived from Figure 4a. Likewise the gradients for $H_2S$ and $SO_2$ were obtained from the concentration versus time plot (Figure 6) derived from Figure 4b. While that for NO, $NO_2$ and $O_3$ were obtained from concentration changes with time plots (Figures 7 and 8) derived from Figure 3c.

The dilution rate was determined with the normalised rate change of the mass fraction of the initial gas concentration in the mixture. If $C_{0,i}$ is the mass concentration of gas $i$ in air before dilution and $C_{t,i}$ the mass concentration of gas in air after dilution, then the mass fraction $y_i$ of the concentrate gas was obtained by:

$$y_{i,t} = \frac{m_{0,i}}{m_{t,i}} = \frac{C_{0,i}V_0}{C_{t,i}V_t} = \frac{C_{0,i}h_s}{C_{t,i}h_n} \tag{5}$$

where $V_o$ and $V_t$ are the nocturnal mixing volume and the mixing volume at any time $t$ after sunrise; the $m_{0,i}$ and $m_{t,i}$ are the mass of gas $i$ at night and at any time $t$ after sunrise; $h_n$ and $h_s$ are the daytime and night time mixed layer heights respectively. Equation (5) provides the mass fraction of a trace gas at any particular time $t$ relative to the initial concentration. The dilution factor, which indicates the extent of dilution, was obtained using the following equation:

$$DF_i = \frac{C_{0,i}}{C_{t,i}} \tag{6}$$

The estimated dilution factor, $DF_{CO}$ for CO was determined as the ratio of the average night time to the daytime concentrations. At $t = 10:00$, $DF_{CO}$ equals 1.7, based on the assumption that the mixture still remained a homogenous mixture with no deposition. The dilution rate $DR_i$ is the product of $-DF_i^{-1}$ and the slope of the plot of $y_{i,t}$ against $t$. It is estimated using the following equation:

$$DR_i = -\frac{1}{DF_i}\left(\frac{dy_{i,t}}{dt}\right) \tag{7}$$

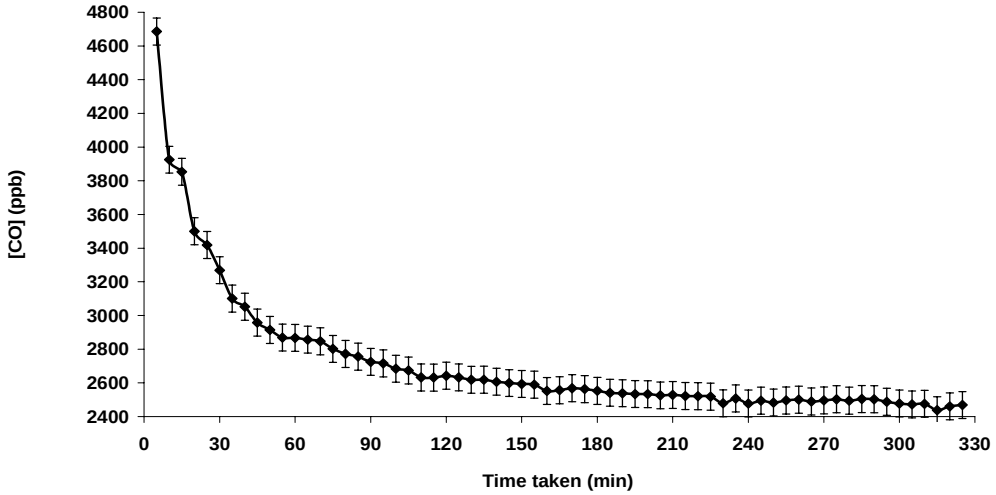


**Figure 5**. The reduction in ambient carbon monoxide concentration as a result of dilution.

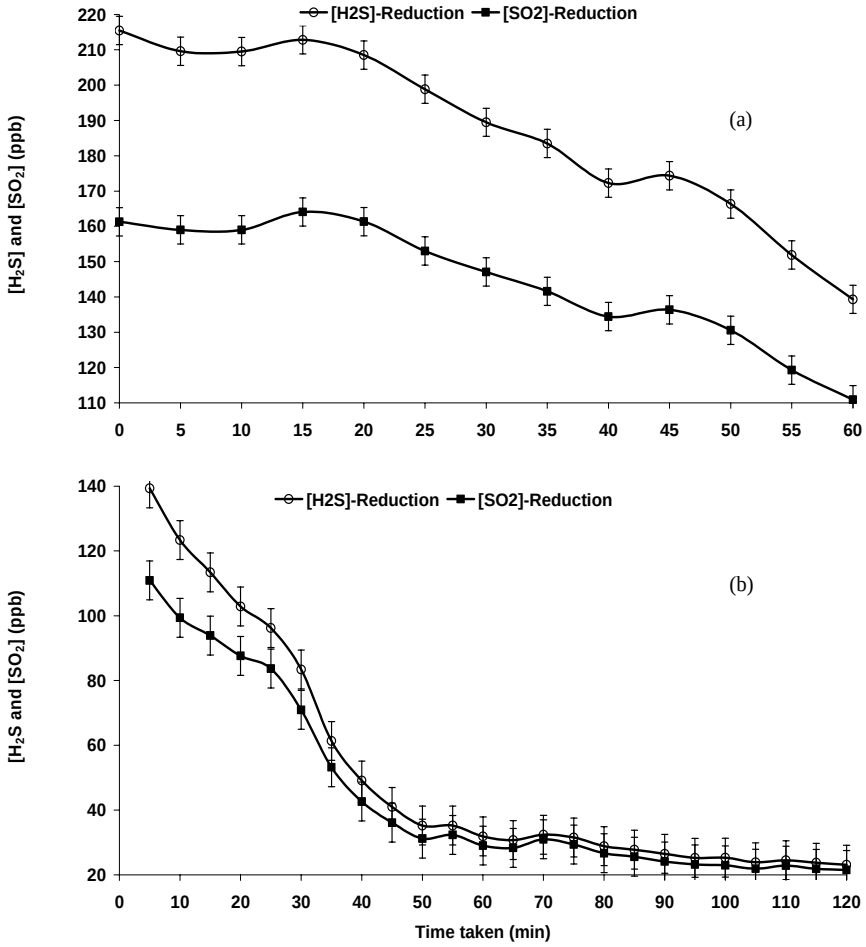


**Figure 6**. The reduction in ambient $H_2S$ & $SO_2$ concentrations as a result of (a) chemical transformation and (b) dilution.

The estimated dilution rates for the other observed trace gases are indicated in Table 2.

**Table 2.** Mean Daily Percentage Reduction by Dilution

| Trace Gases | CO | $O_3$ | $H_2S$ | $SO_2$ | NO | $NO_2$ |
|---|---|---|---|---|---|---|
| $DR$ /$10^{-3}$ min | 1.0 | 1.12 | 2.41 | 2.53 | 2.35 | 1.94 |

### 4.5. Chemical Transformations of the Emitted Gases

The oxidation of $H_2S$ and $SO_2$ from measurements began with a rapid decline in ambient concentration within one hour (Figure 6) at low wind speed of 1 to 2 $m{\cdot}s^{-1}$. The oxidising agent is produced during the chemical transformation of NO (Figure 7) in the presence of volatile organic compounds and sunlight (Moller, 1980; Chisaka, 1984; Warneck, 1999). In order to determine a reaction rate, for convenience the time of day is replaced with the duration of the formation or disappearance episode. The corresponding concentrations show how concentration varies with time until a stable concentration value is attained. The reduction in the intensity of solar radiation with sunset reduces the concentration of the oxidants as well as the photo-oxidation of $H_2S$ and $SO_2$, leading to an increase in the night time concentrations resulting from emissions (Figure 4b).

**Table 3.** Selectivities of Two Oxidants for Photochemical Reactions

| Oxidants | Selectivity (%) |
|---|---|
| NO | 13.16 |
| $O_3$ | 86.84 |

Atmospheric reactions are influenced and propagated by the continuous presence of $O_3$ and other oxidants as well as the oxidant precursors. To ascertain the most significant oxidising agent between $O_3$ and NO with diurnal variations, selectivity of the two compounds were evaluated. Higher selec-

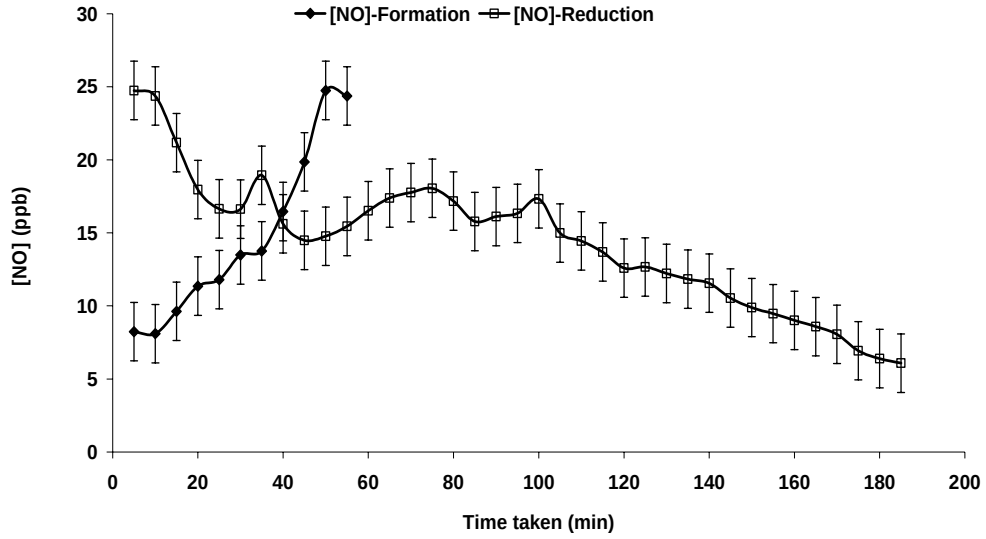


**Figure 7**. The formation and reduction profiles of ambient nitrogen monoxide concentrations between 04:00 and 11:00 as a result of chemical transformation.

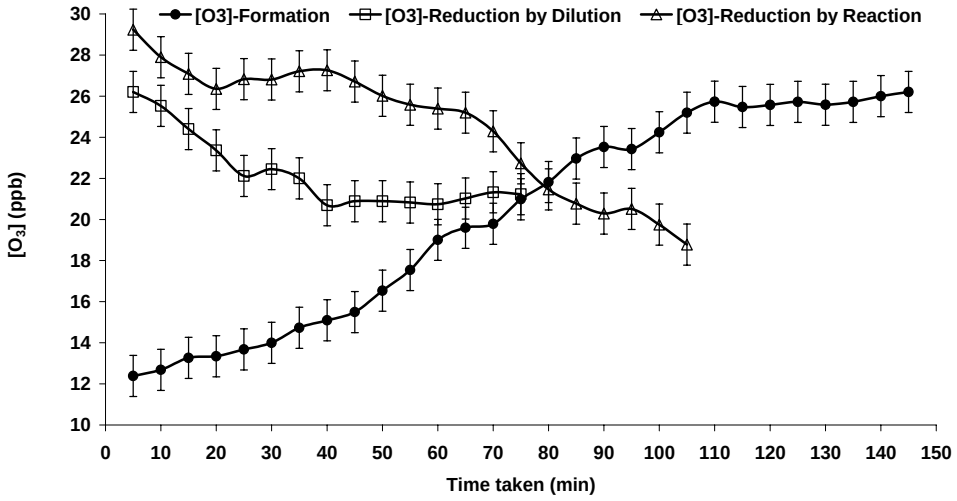


**Figure 8**. The formation and reduction profiles of ambient ozone concentrations from 07:00 to 11:00 and from 15:00 to 17:00 as a result of dilution and chemical transformation.

tivity was observed with $O_3$ (Table 3) as the dominant oxidising agent and its oxidising potential of about 87% is reasonably significant over the surface meteorological conditions (Table 1). Similar observations of $O_3$ oxidising potentials have been reported by Pienaar and Helas (1996).

NO formation and consumption were the first observed daily chemical transformations. The formation is associated with combustion processes, while the consumption occurs simultaneously with the appearance of daylight, hence photo-oxidation. The rate of NO production appears higher than the rate of consumption which implies that the disappearance of $NO_2$ should have a higher rate constant than the disappearance of NO (Figure 7).

The formation of $O_3$ in the troposphere is associated with the presence of sunlight. The formation reaction was impeded by dilution for about one hour followed by accumulation due to reaction. The dilution reduced the concentration between 9:00 and 10:00. This was ascertained based on the assumption that the diluent air introduces oxygen-rich air into the mixture. The presence of excess oxygen in the reaction has no indirect effect since it only increases one of the participating reactants for the ozone production. It is not impossible that $O_3$ formation happened in the diluent air mass but based on the concentration reduction that interfered with the initial daytime concentration profile, the rate plot after the dilution was used in developing the formation rate model expression with its

initial concentration taken as the concentration after dilution (Figure 8).

### 4.6. Dilution Effect on Transformation

It has been shown that a considerable amount of photo-oxidation occurs daily accompanied by dilution near open cast coalmines (Figures 4a to 4c). Apart from CO with average residence time of 2.5 months in the atmosphere, $H_2S$, $SO_2$, $O_3$, NO and $NO_2$ undergo chemical transformation (photo-oxidation) during the day. This photochemical transformation is inhibited by dilution resulting from the increase mid morning wind speed from about 1.5 $m{\cdot}s^{-1}$ to 3.7 $m{\cdot}s^{-1}$. This variation in wind speed produces turbulent mixing of the clean air which traverses the coalmines. The introduction of cleaner air (relatively free of the measured species) created concentration reduction of the observed trace gases that were already experiencing photochemical transformation after sunrise. However the photochemical transformations interfered by the dilution process started again after 11:00 (Figure 4c).

The transformations of $H_2S$, $SO_2$ and $O_3$ were the only processes that were significantly interfered by dilution while NO and $NO_2$ transformations occurred some hours before the observed rise in wind speed (Figures 4b and 4c). Prior to the period that dilution was distinctly observed (09:00 and 11:00), $H_2S$, $SO_2$ and $O_3$ were already experiencing concentration reduction as a result of photochemical oxidation. While between 09:00 and 11:00, the dilution process reduced the $H_2S$ and $SO_2$ concentrations up to levels insufficient to further undergo chemical transformation. But with $O_3$ formation, the dilution only reduced the concentrations but did not terminate the reaction. This was due to the wind speed attaining steady state while solar radiation that propagates ozone formation was not yet at its peak.

The $H_2S$ and $SO_2$ nocturnal concentrations were reduced between 08:00 and 09:00 by about 39% and 38.2% respectively attributed to transformation while about 70% of the remain concentrations were reduced by the dilution between 09:00 to 11:00 (Figure 6a and 6b). In general a total of about 80% of the night time $H_2S$ and $SO_2$ concentrations were reduced during the day.

The chemical transformation involving NO occurred in the morning between 04:00 and 09:00. It was assumed that the NO formation was entirely the result of oxidation during combustion and photo-dissociation of $NO_2$ in the reaction mixture. The formation of NO increased the average night time concentration by approximately 45% between 04:00 and 06:00 and thereafter, decreased exponentially to about 29% of the average night time concentration between 06:00 and 09:00 (Figure 7).

The formation of $O_3$ increased the night time concentration by about 46% between 07:00 and 09:00 due to photochemical oxidation, and then between 09:00 and 11:00, decreased to about 30% of the night time concentration due to dilution (Figure 8). With increased solar radiation $O_3$ increased to about 62% of the night-time concentration between 10:00 and 15:00. The transformation rate was determined from the concentration increase between 07:00 and 09:00.

### 4.7. Rate Models and Temperature Dependent Constants

The rate models developed are expressed in concentration-time relationship of the various trace gas measurements from two predominant wind directional sectors classified as $157.5^o$ to $202.5^o$ and $292.5^o$ to $337.5^o$. These wind sectors were chosen based on the emission source observations (Figures 2a to 2f). The reaction rate was determined with estimated daytime mixing layer height and a constant nocturnal gas concentration. The disappearance of $H_2S$ between 08:40 and 09:40 generated a first-order rate expression given by equation (8). The same was found for $SO_2$ disappearance between 08:40 and 09:40 shown by equation (9). The mean background levels for $H_2S$ and $SO_2$ upwind of the sampling area was as low as 2.9 and 6.5 ppb, which was almost insignificant, compared to the average night time concentrations (Figure 3b) and had a negligible effect on the night time concentrations. The $H_2S$ and $SO_2$ rates in $\mu g{\cdot}L^{-1}\text{min}^{-1}$ was determined from Figure 6, with $[H_2S]$ and $[SO_2]$ being ambient concentrations of the observed hydrogen sulphide and sulphur dioxide respectively, are expressed in equations (8) and (9) below:

$$-\frac{d[H_2S]}{dt} = k_{H_2S}[H_2S]^2 \tag{8}$$

$$-\frac{d[SO_2]}{dt} = k_{SO_2}[SO_2]^2 \tag{9}$$

where $k_{H_2S} = 2.19\times10^{-3}\ L{\cdot}\text{min}^{-1}{\cdot}\mu g^{-1}$ and $k_{SO_2} = 1.45\times10^{-3}\ L{\cdot}\text{min}^{-1}{\cdot}\mu g^{-1}$ are the reaction rate constants for equations. Other kinetic parameters which include the order of reaction ($n$), pre-exponential rate constant ($k_\infty$) and activation energy ($E/R$) over the observed surface ambient temperatures are summarised in Table 4.

The disappearance rate of $NO_2$ was determined from the formation of NO, which occurred between 05:00 and 07:00. The early morning NO and $NO_2$ average background concentrations were approximately 1.2 ppb and 3.0 ppb respectively, which were also insignificant, compared with the average night time concentrations (Figure 3c). The developed rate for $NO_2$ and NO obtained from Figure 7, are given by equations (10) and (11) based on same assumptions made for $H_2S$ and $SO_2$.

$$-\frac{d[NO_2]}{dt} = k_{NO_2}[NO_2] \tag{10}$$

$$-\frac{d[NO]}{dt} = k_{NO}[NO] \tag{11}$$

where $k_{NO_2} = 1.19\times10^{-2}\ \text{min}^{-1}$ and $k_{NO} = 3.55\times10^{-2}\ \text{min}^{-1}$.

The $O_3$ production and consumption occurs during daytime. Its formation and consumption mechanisms have been

**Table 4**. Reaction Kinetic Parameters Estimated for Trace Gases near Open Cast Coalmines

| Parameter | $H_2S$ | $SO_2$ | $NO_2$ | NO | $O_3$ |
|---|---|---|---|---|---|
| Order, $n$ | 1.9 | 2.2 | 1.2 | 0.97 | 2.1 |
| Rate Constant, $k$ at $T_i(K)$ | $2.19 \times 10^{-3}$ $L{\cdot}\mu g^{-1}{\cdot}\min^{-1}$ | $1.45 \times 10^{-3}$ $L{\cdot}\mu g^{-1}{\cdot}\min^{-1}$ | $1.19 \times 10^{-2}$ $\min^{-1}$ | $3.55 \times 10^{-2}$ $\min^{-1}$ | $1.59 \times 10^{-3}$ $L{\cdot}\mu g^{-1}{\cdot}\min^{-1}$ |
| $T_i(K)$ | 285 | 285 | 278 | 283 | 288 |
| $k_\infty$ between $T_1$ and $T_2$ | $6.65 \times 10^{-3}$ $L{\cdot}\mu g^{-1}{\cdot}\min^{-1}$ | $1.67 \times 10^{-2}$ $L{\cdot}\mu g^{-1}{\cdot}\min^{-1}$ | $4.7 \times 10^{-3}$ $\min^{-1}$ | $1.27 \times 10^{-2}$ $\min^{-1}$ | $5.49 \times 10^{-1}$ $L{\cdot}\mu g^{-1}{\cdot}\min^{-1}$ |
| $T_1$ to $T_2$ ($K$) | 282 – 288 | 282 – 288 | 276 – 279 | 279 – 283 | 288 – 293 |
| $E_A/R$ ($K$) | 316.69 | 696.02 | – 258.22 | – 291.72 | 1,683.91 |

described in Warneck (1999), Karol et al., (1997), and Pienaar and Helas (1996). The $O_3$ disappearance rate model evaluated from Figure 8 is given by equation (12).

$$-\frac{d[O_3]}{dt} = k_{O_3}[O_3]^2 \tag{12}$$

where $k_{O_3} = 1.59 \times 10^{-3}\ L{\cdot}\min^{-1}{\cdot}\mu g^{-1}$.

Associated with the above-formulated rate expressions are the temperature dependent reaction rate constants (see Table 4) given in the form of the Arrhenius equations (13) to (17).

$$k_{H_2S} = 6.65x10^{-3}\exp\left[-\frac{316.69}{T(K)}\right],\ L{\cdot}\mu g^{-1}{\cdot}\min^{-1} \tag{13}$$

$$k_{SO_2} = 1.67x10^{-3}\exp\left[-\frac{696.02}{T(K)}\right],\ L{\cdot}\mu g^{-1}{\cdot}\min^{-1} \tag{14}$$

$$k_{NO_2} = 4.7x10^{-3}\exp\left[-\frac{258.22}{T(K)}\right],\ \min^{-1} \tag{15}$$

$$k_{NO} = 1.27x10^{-2}\exp\left[-\frac{291.72}{T(K)}\right],\ min^{-1} \tag{16}$$

$$k_{O_3} = 5.49\times10^{-1}\exp\left[-\frac{1683.91}{T(K)}\right],\ L{\cdot}\mu g^{-1}{\cdot}min^{-1} \tag{17}$$

Equations (13) to (17) are determined decay rate constants of the sampled trace gases in the planetary boundary layer only for ambient temperatures of between 0 and 20 °C and mean surface pressure of 850 mbar coupled with the meteorological conditions given in Table 1. Outside these conditions, the Arrhenius equation is not valid. From equation (14), the calculated $SO_2$ disappearance rate at 14.4 ± 0.6 °C was $2.42 \times 10^{-5}\ s^{-1}$, which closely conforms to the values ranging from $1.3 \times 10^{-4}\ s^{-1}$ to $1.09 \times 10^{-5}\ s^{-1}$ obtained by Prahm et al. (1980); Eggleton and Cox (1978); Ronneau and Snappe-Jacob (1978) and Calvert et al. (1978). Numerical rate constants for the other gases could be obtained from equations (13) to (17) at the given temperature range and mean surface pressure.

## 5. Conclusions

The behaviours exhibited by trace gases evolving within open cast coalmines from spontaneous combustion processes and chemical transformations in Witbank area has been shown. The gases revealed distinct diurnal patterns caused by the variations in meteorological parameters coupled with chemical transformations.

In winter, temperature, relative humidity, solar radiation and rain are usually lower than those in summer. These conditions do not favour atmospheric oxidation especially for the sulphur species (Moller, 1980). In addition, the nocturnal inversions are very common in winter (Saghafi, 2002) as well as low mixing height over the Witbank area. These factors all contribute to the accumulation of pollutants in winter from spontaneous coal combustion in the planetary boundary layer.

The pollution rises have shown the Witbank area to be a significant source of CO, $H_2S$, $SO_2$ and NO due to the presence of open cast coalmines. The $O_3$ and $NO_2$ found within the area are mainly products of atmospheric oxidations. This is concluded because no specific wind directional sector was observed as a targeted source for the latter compounds. Dilution factors and rates were established for all observed trace gases over the same time of day based on wind speed as the controlling agent.

Transformation rates, rate constants and activation energies were estimated for $H_2S$, $SO_2$, $NO_2$, NO and $O_3$ over ambient temperature in winter. The reaction rates were estimated while accounting for dilution between 09:00 and 10:00, reactants background concentrations as well as the assumption that the initial concentration of a reactant was its night time concentration.

**Acknowledgments.** The authors wish to express their appreciation to Dr. K. Ross (Consulting, Research and Development, Eskom Resources and Strategy) for several suggestions made during the preparation of this paper. The authors thank the Climatology Research Group, University of the Witwatersrand, for the use of certain ins-

truments during the field study.

## References


Andrews, J.E., Brimblecombe, P., Jickells, T., Liss, P. and Reid, B. (2004). *An Introduction to Environmental Chemistry*, 2nd Edition, Blackwell Science Ltd., UK.

Barker and Associates (1985). *Coalfields of South Africa*, Johannesburg, South Africa.

Barry, R.G. and Chorley, R.J. (1998). *Atmosphere, Weather and Climate*, 7th Edition, Routledge, London.

Blanchet, J.P. (1995). Mechanism of Direct and Indirect Climate Forcing by Aerosols, Report of the Dahlem Workshop on Aerosol Forcing of Climate, Berlin 1994, pp. 109-121.

Breytenbach, L., Pareen, W.V., Pienaar, J.J. and Eldik, R.V. (1994). The Influence of Organic Acids and Metal Ions on the Kinetics of the Oxidation of Sulphur (IV) by Hydrogen Peroxide, Atmospheric Environment, 28 (15), 2451-2459.

Briggs, G.A. (1969). Plume Rise, U.S. Atomic Energy Commission Division of technical information Pub., Tennessee, USA.

Calvert, J.G., Su, F., Bottenheim, W.J. and Strausz, O.P. (1978). Mechanism of the Homogeneous Oxidation of Sulphur Dioxide in the Troposphere. *Atmos. Environ.*, 12(1-3), 197-226.

Carmichael, G.R. and Peters, L.K. (1984). An Eulerian Transport/Transformation /Removal Model for $SO_2$ and Sulfate-I. Model Development. *Atmos. Environ.*, 18(5), 937-951.

Charlson, R.J., Vanderpol, A.H., Covert, D.S., Waggoner, A.P. and Ahlquist, N.C. (1974). $H_2SO_4/(NH_4)_2SO_4$ Background Aerosol: Optical Detection in St. Louis Region. *Atmos. Environ.*, 8(12), 1257-1267.

Chan, W.H., Vet, R.J., Lusis, M.A., Hunt, J.E. and Stevens, R.D.S. (1980). Airborne Sulfur Dioxide to Sulfate Oxidation Studies of the INCO 381M Chimney Plume. *Atmos. Environ.*, 14(10), 1159 -1170.

Chisaka, F. (1984). *Bulletin of the Journal of Society of Mechanical Engineers*, 27(228), 1-22.

Cimorelli, A.J., Perry, S.G., Venkatram, A., Weil, J.C., Paine, R.J., Wilson, R.B., Lee, R.F., Peters, W.D., Brode, R.W. and Paumier, J.O. (2004). *AERMOD: Description of Model Formulation*, US EPA Office of Air Quality Planning and Standards Emission Monitoring and Analysis Division, North Carolina.

Cox, R.A. and Sandalls, F.J. (1974). The Photo-Oxidation of Hydrogen Sulphide and Dimethyl Sulphide in Air. *Atmos. Environ.*, 8 (12), 1269-1271.

Davison, G. and Hewitt, C.N. (1997). *Air Pollution in the United Kingdom*, The Royal Society of Chemistry, London.

Deardorff, J.W., Villis, G.E. and Stockton, G.H. (1980). Laboratory studies of the entrainment zone of a convectively mixed layer. *J. Fluid Mech.*, 100, 41-64.

Dittenhoefer, A.C. and De Pena, R.G., Dittenhoefer, A.C. and de Pena, R.G. (1978). A study of production and growth of sulfate particles in plumes from a coal-fired power plant. *Atmos. Environ.*, 12(1-3), 297-306.

Edna, P. (1957). *Coal in Southern Africa*, University Press, University of the Witwatersrand, Johannesburg, South Africa.

Eggleton, A.E.J. and Cox, R.A. (1978). Homogeneous Oxidation of Sulphur Compounds in the Atmosphere. *Atmos. Environ.*, 12 (1-3), 227-230.

Felder, R.M. and Rousseau, R.W. (2000). *Elementary Principles of Chemical Processes*, 3rd Edition, John Wiley, New Jersey.

Fugas, M. and Gentilizza, M. (1978). The Relationship between Sulphate and Sulphur dioxide in Air. *Atmos. Environ.*, 12(1-3), 335-337.

Garratt, J.R. (1992). *The Atmospheric Boundary Layer*, Cambridge University Press.

Gayer, R. and Harris, I. (Ed.) (1996). *Coalbed Methane and Coal Geology*, Geological Society, London.

Gillani, V.N., Husar, R.B., Husar, J.D., Petterson, D.E. and Wilson, W.E. (1978). Project mistt: Kinetics of particulate sulfur formation in a power plant plume out to 300 km, *Atmos. Environ.*, 12(1-3), 589-598.

Gillani, N.V. and Wilson, W.E. (1983). Gas-To-Particle Conversion of Sulphur in Power Plant Plumes-II. Observations of Liquid-Phase Conversions. *Atmos. Environ.*, 17(9), 1739-1752.

Hanna, S.R. and Chang, J.C. (1993). Hybrid plume dispersion model (HPDM), improvements and testing at three field sites. *Atmos. Environ.*, 27A(9), 1491-1508.

Hanna, S. R., and Paine, R. J. (1987). Convective Scaling Applied To Diffusion of Buoyant Plumes from Tall Stacks, Atmospheric Environment, 21(10), 2153 – 2162.

Held, G., Gore, B.J., Surridge, A.D., Tosen, G.R., Turner, C.R. and Walmsley, R.D. (Eds.) (1996). *Air Pollution and its Impacts on the South African Highveld*, Environmental Scientific Association, Cleveland, South Africa.

Holtslag, A.A.M. and Van Ulden, A.P. (1983). A simple scheme for daytime estimates of the surface fluxes from routine weather data. *J. Clim. Appl. Meteorol.*, 22(4), 517-529.

Karol, I.L., Ozolin, Y.E. and Rozanov, E.V. (1997). Box and Gaussian plume models of the exhaust composition evolution of the subsonic transport aircraft in and out of the flight corridor. *Ann. Geophysicae*, 15, 88-96.

Levenspiel, O. (1999). *Chemical Reaction Engineering*, 3rd Edition, John Wiley and Sons Inc, New York.

Liberti, A., Brocco, D. and Possanzini, M. (1978). Adsorption and Oxidation of Sulphur dioxide on particles. *Atmos. Environ.*, 12 (1-3), 255-261.

McGonigle, A.J.S., Thomson, C.L., Tsanev, V.I. and Oppenheimer, C. (2004). A simple technique for measuring power station $SO_2$ and $NO_2$ emissions. *Atmos. Environ.*, 38, 21-25.

Miller, D.F. (1978). Precursor effects on $SO_2$ Oxidation. *Atmos. Environ.*, 12(1-3), 273-280.

Moller, D. (1980). Kinetic model of atmospheric $SO_2$ Oxidation based on published data. *Atmos. Environ.*, 14, 1067-1076.

Oke, T.R. (1987). *Boundary Layer Climates*, 2nd Edition, Methuen and Co. Inc, New York.

Panofsky, H.A. and Dutton, J.A. (1984). *Atmospheric Turbulence: Models and Methods for Engineering Applications*, John Wiley & Sons, New York.

Pasquill, F. (1974). *Atmospheric Diffusion*, 2nd Edition, Ellis Horwood, Ltd., Chichester, England.

Perry, R.H. and Green, D.W. (1998). *Perry's Chemical Engineer's Handbook*, McGraw Hill Book Co. International Edition, 7th Edition, Singapore.

Pienaar, J.J. and Helas, G. (1996). The Kinetics of chemical processes affecting acidity in the atmosphere. *S. Afr. J. Sci.*, 92, 128-132.

Prahm, L.P., Conradson, K. and Nielsen, L.B. (1980). Regional source quantification model for Sulphur Oxides in Europe. *Atmos. Environ.*, 14(9), 1027-1054.

Rodhe, H. (1978). Budgets and turn-over times of atmospheric Sulphur compounds. *Atmos. Environ.*, 12, 671-680.

Ronneau, C. and Snappe-Jacob, N. (1978). Atmospheric transport and transformation rate of Sulphur dioxide. *Atmos. Environ.*, 12(6-7), 1517-1521.

Saghafi, A. (2002). *Environmental and Greenhouse Gas Emissions from Open Cut Mines*, CSIRO Energy Technology.

Santos, C.Y.M., Azevedo, D.A. and Aquino-Neto, F.R. (2004). Atmospheric distribution of organic compounds from urban areas near a coal-fired power station. *Atmos. Environ.*, 38, 1247-1257.

Selvam, A.M., Ramachandra Murty, A.S., Manohar, G.K., Kandalgaonkar, S.S. and Ramana Murty, Bh.V. (1984). *Proc. VII Inter-*

*national Conference on Atmospheric Electricity*, *American Meteorological Society*, pp. 154-159.

Smith, J.M., Van Hess, H.C., Abbott, M.M. (1996). *Introduction to Chemical Engineering Thermodynamics*, 6th Edition, McGraw-Hill, New York.

Seinfeld, J.H. and Pandis, S.N. (1998). *Atmospheric Chemistry and Physics: From Air Pollution to Climate Change*, Wiley Interscience, New York.

Snyman, G.M., Held, G. and Brassel, K.M. (1990). Vertical profiles of particulates on the South Africa highveld, *1st IUAPPA Regional Conference on Air Pollution Towards the 21st Century Implications, Challenges, Options and Solutions*, 1(52), 1-17.

Stockwell, W.R. (1986). A homogeneous gas phase mechanism for use in a regional acid deposition model. *Atmos. Environ.*, 20(8), 1615-1632.

Tang, I.N., Wong, W.T. and Munkelwitz, H.R. (1981). The relative importance of atmospheric Sulphates and Nitrates in visibility reduction. *Atmos. Environ.*, 15(12), 2463-2471.

Terblanche, A.P.S., Danford, I.K. and Nel, C.M.E. (1993). Household energy use in South Africa, air pollution and human health. *J. Energy South Africa*, 54-57.

Timko, R.J. and Derrick, R.L. (1989). *Detection and Control of Spontaneous Heating in Coal Mine Pillars: A Case Study*, US Bureau of Mines.

Twomey, S. (1991). Aerosols Cloud and Radiation. *Atmos. Environ.*, Part A, 25, 2435-2442.

Van Ulden, A.P. and Holtslag, A.A.M. (1985). Estimation of atmospheric boundary layer parameters for diffusion applications. *J. Clim. Appl. Meteorol.*, 24, 1196-1207.

Venkatram, A. (1980a). Estimating the Monin-Obukhov length in the stable boundary layer for dispersion calculations. *Bound. -Layer Meteorol.*, 19, 481-485.

Venkatram, A. (1980b). Dispersion from an elevated source in a convective boundary layer. *Atmos. Environ.*, 14, 1-10.

Walcek, C.J., Brost, R.A., Chang, J.S. and Wesley, M.L. (1986). $SO_2$, Sulphate and $HNO_3$ deposition velocities computed using regional landuse and meteorological data. *Atmos. Environ.*, 20(5), 949-964.

Warneck, P. (1999). The relative importance of various pathways for the Oxidation of Sulphur Dioxide and Nitrogen Dioxide in sunlit continental fair weather clouds. *Phys. Chem. Chem. Phys.*, 1, 5471-5483.

WHO (1979). *Environmental Health Criteria 7: Photochemical Oxidants*, United Nations Environ, Programme Geneva.

Wyngaard, J.C. (1988). Structure of the PBL, Lectures on Air-Pollution Modelling, in A. Venkatram and J.C. Wyngaard (Eds.), *American Meteorological Society*, pp. 9-61.

Zib, P. (1977). *Urban Air Pollution Dispersion Models: A Critical Survey*, Published by Department of Geography and Environmental Studies, University of the Witwatersrand.

Zilitinkevich, S.S. (1972). On the determination of the height of the Ekman Boundary-layer. *Bound.-Layer Meteorol.*, 3, 141-145.